
Biogeochemistry **71:** 415–436, 2004.

Spatial and temporal simulation of soil CO_2 concentrations in a small forested catchment in Virginia

DANIEL L. WELSCH[1,2,*] and GEORGE M. HORNBERGER[1]

*[1]Department of Environmental Sciences, University of Virginia, P.O. Box 400123, Charlottesville, VA 22904, USA; [2]Current address: Department of Geography, Frostburg State University, Frostburg, MD 21532, USA; *Author for correspondence (e-mail: dwelsch@frostburg.edu; phone: +1-301-687-4891; fax: +1-301-687-4495)*

Received 7 October 2002; accepted in revised form 12 March 2004

Key words: Carbon dioxide, Catchment, Physically-based model, Spatial variation

Abstract. The question of how to extrapolate point measurements of soil CO_2 processes to coarser scales remains unanswered because we know little about the spatial and temporal variability in the CO_2 concentration of soil air. In this work, we describe a series of simple physically-based models that simulate soil temperature, soil tension, and soil CO_2 processes. We apply these models to simulate the spatial and temporal dynamics of soil CO_2 concentrations throughout a small catchment in the Virginia Blue Ridge. Output from the simulations is compared with field measurements. We find that despite some model deficiencies, we are able to simulate the gross patterns through space and time of soil air CO_2 concentration. During the growing season when soil temperature is high, we find that soil water status is the limiting control on soil respiration and CO_2 concentration. We also find that soil CO_2 concentration can be high despite low respiration values due to decreased soil diffusivity as moisture fills pore spaces.

Introduction

The inorganic C cycle in forest soils has been identified as playing a key role in many terrestrial and aquatic processes across large spatial and temporal gradients, from setting local soil water alkalinity to affecting global climate change (McFee and Kelly 1995). However, little information exists on the spatial and temporal dynamics of this important component of the C cycle. The mechanisms and rates of CO_2 production (respiration) and resultant concentration are complex. In addition, they vary greatly through both time and space. Because of this large variation, the question of how to use point measurements to make inferences at larger scales is vexed (Rout and Gupta 1989; Fang et al. 1998).

Soil temperature and soil moisture are two main factors controlling soil respiration (Orchard and Cook 1983; Howard and Howard 1993; Lomander et al. 1998; Fang and Moncrieff 2001). Both of these factors vary predictably through space and time. Soil temperature varies diurnally and annually, and spatially with elevation, depth, and vegetation cover type and density. Soil moisture varies temporally according to rainfall and evapotranspiration, and spatially with variation in topography, vegetation, and soil characteristics. This variation is at least partially

predictable and can be described mathematically (Western et al. 1999; Kang et al. 2000). Other factors that influence CO_2 production vary through space and time in a less predictable manner. These include soil organic carbon concentrations, soil bulk density, characteristics of microbial populations, fine root density, and soil pH.

Because the spatial and temporal variation in soil temperature and soil moisture is predictable, these factors can be simulated. Soil temperature can be simulated using energy balance approaches (Thunholm 1990), empirical relationships, heat-transfer relationships (Vose and Swank 1991), or hybrid approaches combining two or more of the others (Kang et al. 2000). Soil moisture patterns can be simulated using Richard's equation, empirical relationships with rainfall or topography (Western et al. 1999), simple bucket models, or hybrid approaches.

The issue of upscaling models from point to catchment and larger scales is unresolved. Models that are capable of simulating spatial and temporal dynamics of soil moisture and soil temperature have been developed, as have models capable of predicting soil respiration, soil CO_2 concentrations, and soil efflux (Šimůnek and Suarez 1993; Fang and Moncrieff 1999). Linkage of these models to simulate the variation of soil CO_2 processes through space and time is one approach for addressing the upscaling problem and that is what we attempt in this paper.

Mathematical models of CO_2 production and transport have typically been run through time for one point using measured data as inputs (Šimůnek and Suarez 1993; Fang and Moncrieff 1999). Our work is unique because we simulate spatial and temporal variability of the input data using mathematical models and then use the simulated forcing functions to run the model of CO_2 processes through both space and time. In this paper, we introduce a series of linked mathematical models that are capable of adequately simulating the spatial and temporal dynamics of CO_2 in forest soils throughout a small catchment in Virginia. We find that soil CO_2 concentrations are highest in warm soils in the moist hollows, and that during the growing season when soils are warm, soil moisture is the dominant control on respiration. We also find that soil CO_2 concentrations can be episodically high in the absence of high respiration rates due to decreases in gaseous diffusion because of soil wetting.

A limitation of the model presented here is the lack of distributed data on input parameters. Many parameters which are known to vary through space are considered in this first approach to be static. We did this because we chose to put our efforts into developing the ideas upon which the model is constructed rather than to obtain detailed distributed field data. Because of this choice, methodology used in the model is sound and when distributed data become available, it will be easily incorporated into the model structure.

Field site

We developed a model as described below and applied it to the South Fork Brokenback Run catchment, a small (237 ha), mountainous catchment in the Shenandoah National Park, Virginia. The catchment has an elevation range of

525 m, and is completely forested with the exception of a Park Service fire road that roughly parallels the stream. The catchment has been described in more detail by Scanlon et al. (2001).

The mathematical model

Soil temperature model

Soil temperature has been shown to control soil CO_2 production and efflux on both short (daily) and long (seasonal) scales (Howard and Howard 1993; Winkler et al. 1996; Davidson et al. 1998; Fang and Moncrieff 2001). To simulate temperature variation, we adopted the model developed by Kang et al. (2000) that uses a hybrid physical–empirical technique. This model was developed to predict spatial and temporal variation in soil temperature in forested regions, incorporating the effects of topography, canopy cover, and ground litter. The model is based on the heat transfer equation for soil

$$\frac{\partial T}{\partial t} = \frac{\lambda}{\rho c}\frac{\partial^2 T}{\partial z^2} \tag{1}$$

where T is soil temperature, t is time, λ the thermal conductivity, ρ the soil bulk density, c the specific heat capacity of soil and z is the soil depth. The equations used to determine soil temperature through space (including z) and time are, for when $A_j > T_{j-1}$

$$T_j(z) = T_{j-1}(z) + \left[A_j - T_{j-1}(z)\right]\exp\left[-z\left(\frac{\pi}{k_s p}\right)^{1/2}\right]\exp\left[-k\left(\mathrm{LAI}_j + \mathrm{Litter}_j\right)\right] \tag{2}$$

and when $A_j \leq T_{j-1}$

$$T_j(z) = T_{j-1}(z) + \left[A_j - T_{j-1}(z)\right]\exp\left[-z\left(\frac{\pi}{k_s p}\right)^{1/2}\right]\exp\left[-k * \mathrm{Litter}_j\right] \tag{3}$$

where A_j is the average daily air temperature, T_{j-1} is the soil temperature on the previous day, z is depth into the soil, k_s the thermal diffusivity, and p the period of annual temperature variation (seconds). Litter_j is the leaf area index (LAI) equivalent for ground litter, and k is the Beer–Lambert extinction coefficient for radiation in a canopy. Input data required by the model include air temperature, soil thermal properties, LAI, LAI equivalent for litter, and topography (used to scale air temperature). Air temperature (A_j) is scaled with elevation according to an average lapse rate determined through analysis of meteorological data from Sperryville, VA (<10 km from the study site, elevation 375 m) and Big Meadows, VA (<2 km from the study site, elevation 703 m). With the exception of topography, all other input data into the model are considered to not vary through space. LAI varies as an annual sine curve between input minimum and maximum LAI values. See Kang et al. (2000) for a complete description of the model.

Soil tension model

The amount of water contained in the soil can affect both the production and concentration of CO_2 (Šimůnek and Suarez 1993; Fang and Moncrieff 1999). Moisture can enhance or inhibit the metabolic process of respiration and can also affect the concentration of CO_2 in soils by changing the physical properties influencing diffusion of gas from the soil to the atmosphere.

Modeling the spatial and temporal patterns of soil water in a catchment is extremely difficult. On a coarse scale, we know, for example, that hollows will be wetter than ridges, especially following a storm; that is, we expect topography to be a dominant factor in controlling soil moisture distribution. The rainfall-runoff model TOPMODEL is based on the hypothesis that topographically similar areas will respond with hydrological similarity (Beven and Kirkby 1979). Topographic similarity is determined using the topographic index, defined as

$$\mathrm{TI} = \ln \frac{a}{\tan \beta} \tag{4}$$

where a is the upslope contributing area and (tan β is the local slope angle. The index produces temporally static high values in wet locations such as hollows and stream networks and low values for dry locations such as steep slopes and ridge tops. We use a version of TOPMODEL that simulates a shallow stormflow zone and a relatively deeper groundwater zone (Scanlon et al. 2001). Water balance calculations in TOPMODEL determine a saturation deficit, or depth of water that would need to be added to each pixel to saturate it, for each topographic index class for each day in the simulation for both the stormflow zone (shallow soil) and the groundwater zone (deeper soil). To most accurately simulate gravity drainage of water from soils, we used the groundwater saturation deficit because the drainage exhibited in the stormflow zone saturation deficit was very rapid, indicating either wet soils during and immediately following a storm, and dry soils all other times. The groundwater saturation deficit represents drainage of water from the soil following a storm event and is more closely related to measured soil tension. We make use of the timing and magnitude of changes in the saturation deficit to guide our estimation of soil water status by relating saturation deficit to tension.

We first chose values for the lowest and highest maximum daily tensions seen in the catchment through the study period. The highest maximum tension can be thought of as the tension measured at the driest spot in the catchment on a very dry day, and the lowest maximum tension can be considered to be the tension at the same spot on a very wet day. The maximum tension is scaled with the daily catchment average saturation deficit, such that a day with the lowest catchment average saturation deficit (wet soils) would have a maximum tension equal to the lowest maximum tension. On a day with the highest catchment average saturation deficit (dry soils), the maximum tension in the catchment would be equivalent to the highest maximum tension value. The minimum bounds on tension are set at zero (saturation); tension equals zero when saturation deficit equals zero.

Once the possible maximum tension in the catchment for each day is known, the tension at each location in the catchment is determined through a non-linear relationship with the local saturation deficit. The lower bounds for the interpolation are the same as for determining the maximum tension, tension = 0 when saturation deficit = 0. The upper bound for saturation deficit is the maximum saturation deficit calculated in the catchment on that day, and the upper bound for tension is the calculated maximum tension described above. Therefore, the minimum saturation deficit (always 0, in the stream channel) will have a tension of zero and the maximum saturation deficit will have a tension equivalent to the maximum tension determined based on the average saturation deficit of the catchment on that particular day. Soil tension is assumed to be homogenous through the profile being simulated.

Soil CO_2 production and transport model

We adapted the model of Fang and Moncrieff (1999), in which soil pCO_2 is predicted from calculations of below ground respiration rates and CO_2 efflux from the soil surface. The basis of the model is a one-dimensional mass balance for CO_2 in an arbitrary volume assuming there is little horizontal loss or gain of CO_2;

$$\frac{\partial C_t}{\partial t} = -\frac{\partial}{\partial z}\left(F_{dg} + F_{ag} + F_{dw} + F_{aw}\right) + S \tag{5}$$

where F_{dg} and F_{dw} are dispersive/diffusive fluxes in the gaseous and liquid phases of the soil respectively, F_{ag} and F_{aw} are the advective fluxes resulting from gas convection and vertical water movement respectively, S is a depth-dependent term defining sources and sinks of CO_2 in the soil, and C_t is the total CO_2 in both gas and liquid phases. The gaseous flux term in (5) F_{dg} can be defined using Fick's first law:

$$F_{dg} = -D_{gs}\frac{\partial C_g}{\partial z} \tag{6}$$

where D_{gs} is the effective diffusion coefficient of CO_2 in soil. The diffusive flux in the liquid phase (F_{dw}) is usually negligible because the diffusivity of CO_2 through a liquid is about 10,000 times lower than that in the gas phase (Fang and Moncrieff, 1999). The advective flux in the gas phase (F_{ag}) is also negligible because of the slow movement of the soil atmosphere. The advective flux in the liquid phase is defined as

$$F_{aw} = q_w C_w \tag{7}$$

where q_w is the mass flux of water as determined by a simple water balance and C_w is the CO_2 concentration in the liquid phase.

The production of CO_2 in the soil is the result of microbial and root respiration, R_m and R_r respectively. In (5) above, the source/sink term S is defined as:

$$S = R_r + R_m \tag{8}$$

Under the assumption that all organic matter will ultimately be oxidized to CO_2, the microbial respiration rate R_m becomes

$$R_m = \alpha \frac{dM}{dt} = \gamma_m M' \tag{9}$$

where α is a coefficient for the amount of CO_2 given off from decomposition per unit of dry organic matter, M is the amount of substrate available for decomposition, γ_m is the microbial respiration rate parameter of the fine root fraction, and M' is the amount of labile organic matter expressed as an amount of fine roots. Because of the variation in the respiration rates of microbes on dead roots of different sizes, dead root biomass is simplified to an equivalent mass of fine roots, thus requiring only one rate constant (Fang and Moncrieff 1999). Root respiration is a function of root respiration rate and the root biomass. Root respiration (R_r) can be described by

$$R_r = \sum \gamma_{r_i} B_i \tag{10}$$

where γ_{r_i} is the respiration rate parameter for root size class i and B_i is the biomass of size class i. Equations (9) and (10) can be added together and integrated through the soil profile to determine the total CO_2 production.

The respiration rate parameters γ_m and γ_r are dependent upon environmental factors such as temperature, oxygen content in the soil air, and soil moisture conditions. These parameters are determined by assigning an optimal respiration rate at a given temperature (10 °C) and then scaling that value based on the functions of temperature, moisture, and oxygen concentration according to

$$\gamma_r = \gamma_{r0} f(T) f(W) f(O_2) \tag{11a}$$

$$\gamma_m = \gamma_{m0} f(T) f(W) f(O_2) \tag{11b}$$

where γ_r is the root respiration rate, γ_{r0} is the optimal root respiration rate, γ_m is the microbial respiration rate, γ_{m0} is the optimal microbial respiration rate, and $f(T)$, $f(W)$, and $f(O_2)$ are the functions of soil temperature, soil tension, and soil oxygen content, respectively.

The role that temperature plays on the respiration parameters in Equation (11) can be represented using an Arrhenius relationship of the form

$$f(T) = \exp\left(\frac{-E}{RT}\right) \tag{12}$$

where E is the activation energy for respiration, R is the universal gas constant, and T is the absolute temperature.

Moisture affects CO_2 concentrations by changing the diffusional properties of the soil and by altering the metabolic activity of the roots and microbes. Adding water to a dry soil will increase the respiration rate until a certain point, after which the rate will decrease. This can be represented by two equations which represent either

the dry or wet end of the continuum:

$$f(w) = \frac{\log|h| - \log|h_1|}{\log|h_2| - \log|h_1|} \quad h \in (h_2, h_1) \tag{13a}$$

$$f(w) = \frac{\log|h| - \log|h_3|}{\log|h_2| - \log|h_3|} \quad h \in (h_3, h_2) \tag{13b}$$

$$f(w) = 0 \quad h \in (-\infty, h_3) \cup (h_1, +\infty) \tag{13c}$$

where h_2 is the tension where CO_2 production is optimal, h_3 is the tension where respiration ceases because conditions are too dry, and h_1 is the tension where respiration ceases because soils are too wet (Šimůnek and Suarez 1993). Exchange between the dissolved and gaseous forms of CO_2 is regulated by Henry's Law.

At low O_2, increasing the O_2 content of the soil atmosphere increases respiration rapidly but at high values of O_2, there is little effect. A Michaelis–Menten relationship can be used to model this:

$$f(O_2) = \frac{1}{1 + K_M/[O_2]} \tag{14}$$

where K_M is the Michaelis–Menten constant and $[O_2]$ is the concentration of oxygen in the soil air. Oxygen concentrations in soil air are simulated using the method described by Campbell (1985).

Sequence of calculations

The spatial and temporal patterns of CO_2 are simulated by first modeling soil temperature on a daily time step for each pixel (30 m × 30 m) in the watershed for each day in the simulation. Next, TOPMODEL is run to get saturation deficit values and tensions are calculated according to the procedure described above. Finally, soil temperature and soil tension are input into the CO_2 model and respiration rate, concentration, and efflux are calculated for each of five soil layers (including litter layer) specified in each pixel in the watershed for each day of the simulation. TOPMODEL is run on a 15 min time step and then the saturation deficit results are averaged to daily data. The other models are run on a daily time step for a 118 day period beginning on 1 August 2001 and ending on 27 November 2001, coinciding with the time period in which field measurements were made at the 10 sites noted in Figure 1. The model was run for each pixel in the watershed for a 35 day period between 28 August 2001 and 1 October 2001.

Field data collection

Field data for calibration and validation of the coupled models were collected from the South Fork Brokenback Run catchment, located on the East side of the Blue Ridge in the Shenandoah National Park, Virginia. Soil CO_2 concentrations were

monitored every 15 min using a portable infrared gas analyzer (IRGA, PP Systems, EGM-3) at one site near the outlet of the catchment at a depth of 20 cm throughout the length of the study. At 9 other sites in the catchment, CO_2 concentrations were measured weekly at both 20 and 70 cm depth using the same portable IRGA. Soil air pCO_2 was measured according to the methods described in Andrews and Schlesinger (2001) where a soil gas well consisting of 5.25 cm ID PVC pipe cut 20 cm long is inserted vertically into a hole augured to the depth of interest (20 and 70 cm in this study). The top of the PVC pipe is capped with a rubber stopper through which pass two pieces of plastic tubing which extend above the soil surface. It is assumed that the air in the gas well has the same CO_2 concentration as air contained in the soil matrix. The IRGA with integral pump was placed in the loop of the gas well so that air was pumped from the gas well, passed through the IRGA, and pumped back into the gas well. In this way, no pressure changes were induced in the gas well which would affect the concentration of soil air. The tubes extending from the soil surface were capped when measurements were not being made, preventing efflux between measurements. Soil tension, air temperature, and soil temperature were measured every 15 min immediately adjacent to the continuous soil CO_2 measurement site. Tension was measured using a tensiometer coupled to a pressure transducer recorded by a digital datalogger and temperatures were measured using a thermisters recorded by a digital data logger.

Model calibration and sensitivity analysis

The models for soil temperature, soil tension, and soil CO_2 were calibrated individually to fit the continuous data measured at site 1 (Figure 1), and the calibrated model was then applied to the rest of the catchment. For the soil temperature model, thermal diffusivity (k_s) and leaf area index (LAI) were the parameters varied in order to achieve the best fit to the measured data. The value of k_s used is 6×10^{-3} cm^2 s^{-1}, and LAI varied according to a sine function with a minimum of 0 (winter) and a maximum of 4 (m^2 m^{-2}) (summer). These relatively low values represent the conditions at site 1, where the forest canopy is characterized by blowdowns and gaps, including a large gap for the stream. Litter LAI equivalent varies throughout the year with an autumn maximum (4) and a late summer minimum (2.4). Scanlon et al. (2001) calibrated TOPMODEL to measured flow rates at South Fork Brokenback Run; we used their calibrated model. The tension model was calibrated by changing the minimum–maximum and maximum–maximum tensions seen in the catchment throughout the study. We used values of 7 and 400 cm of water respectively in the simulations presented here. The CO_2 portion of the model was calibrated by adjusting two different sets of parameters. The first set is the respiration rate coefficients that define the optimal rates for root and microbial respiration at 10 °C. The values used in this study are 12×10^{-6} and 12×10^{-5} mg CO_2 g dry soil^{-1} s^{-1} for microbial and root respiration, respectively. The values used to simulate the effect of moisture on respiration are 1, 25, and 400 cm H_2O for h_1, h_2, and h_3, respectively (Eq. (13)). These values were

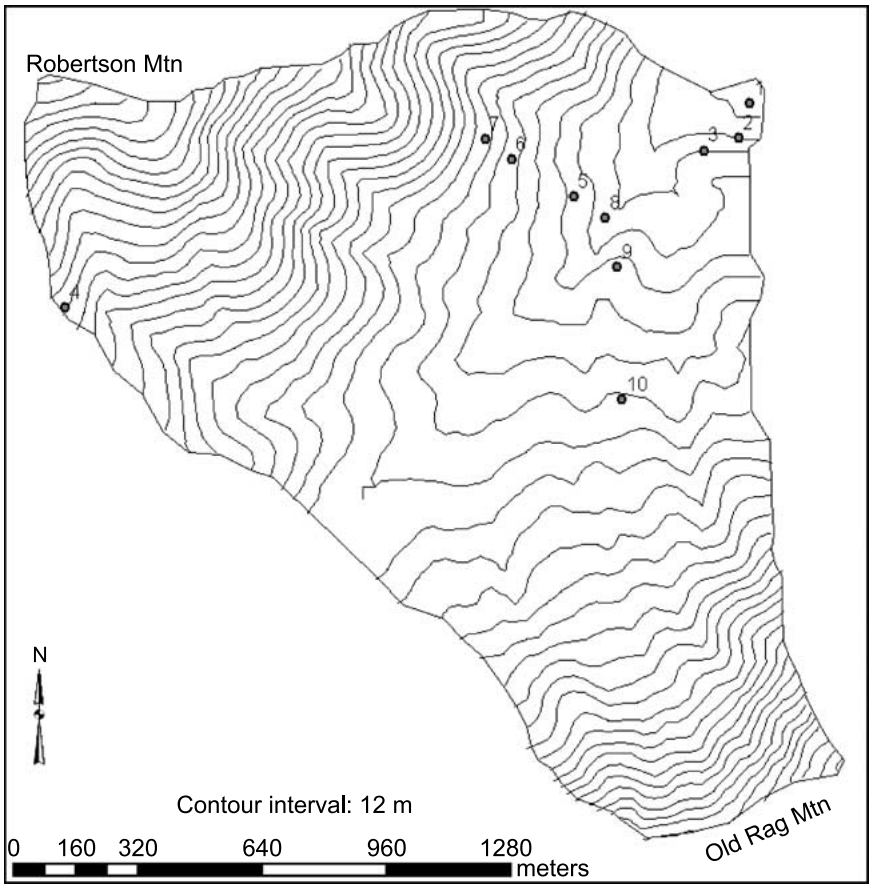

Figure 1. Location map for SFBR watershed. Numbered points indicated are gas well measurement locations.

determined through analysis of observed tension and observed CO_2 concentration data during the growing season when soil temperature was not limiting. Table 1 details the soil properties used in the CO_2 model. Values for root, litter, and organic matter mass were not measured. They were obtained through reasonable estimates in the field in comparison with literature values. Given that we are using a spatial model and that C sources vary widely throughout the catchment, it was futile to sample for these parameters unless we were to undertake a completely distributed analysis of organic C sources within the catchment.

Because we are using models that have been developed previously, complete sensitivity analyses of these models has been performed by their respective authors. For the soil temperature model, readers are referred to Kang et al. (2000), and for the CO_2 model, to Suarez and Šimůnek (1993) and by Moncrieff and Fang (1999). There are only two parameters in the soil tension model; the largest and smallest maximum

Table 1. Soil properties by layer used in CO_2 model. Litter includes all organic matter exclusive of root material.

Layer	Layer thickness (cm)	Bulk density (g/cm^3)	Litter (g/m^2)	Dead roots (g/m^2)	Live roots (g/m^2)
1	5	0.5	600	0	0
2	10	1.5	350	450	910
3	10	1.2	250	165	540
4	5	1.1	150	135	140
5	30	1.2	20	60	50

tensions seen in the catchment throughout the simulated period. The model is extremely sensitive to these parameters, but the range of reasonable parameter values is small for a humid forested watershed, and within this range, variability is limited.

Results

Soil temperature

Soil temperature was simulated on a daily time step for each pixel in the watershed. For the continuously recorded location, the model output for that pixel appears to somewhat underpredict the temperatures when soils are less than about 18 °C and overpredict temperatures greater than about 20 °C (Figure 2A). For the period from August to December 2001 (Figure 2B), the average error (simulated − observed) is −0.3 °C and the Nash–Sutcliffe criterion for goodness of fit is 0.93. The fit is not as good for the spatially distributed data collected weekly (Figure 3). For August to December 2001, the average error is −1.1 °C and the Nash–Sutcliffe criterion for goodness of fit is 0.50 for weekly soil temperatures measurements across the 10 sites in Figure 1. Soil temperature at site 4 is under predicted throughout the entire study. There are no sites which are systematically over predicted.

Soil tension

The model for soil tension overpredicts low tension values (wet soils) by up to 7 cm and underpredicts high tension values (dry soils) by roughly the same amount (Figure 4A). The average error (simulated−observed) for the period is 8.9 cm of water and the Nash–Sutcliffe criterion is −14.5. The extremes in the data are never fully captured, as seen on 13 August when the soil becomes near saturated, but the model predicts a tension of 7 cm, and on 23 September, the driest day in the record, when the measured soil tension was 33 cm, and the model predicted 20 cm (Figure 4B). After about 15 October, the soils remain relatively wet although the model simulates very dry conditions (Figure 4B). If data after this time are not considered, the average error becomes 0.7 cm and the Nash–Sutcliffe criterion increases to 0.77.

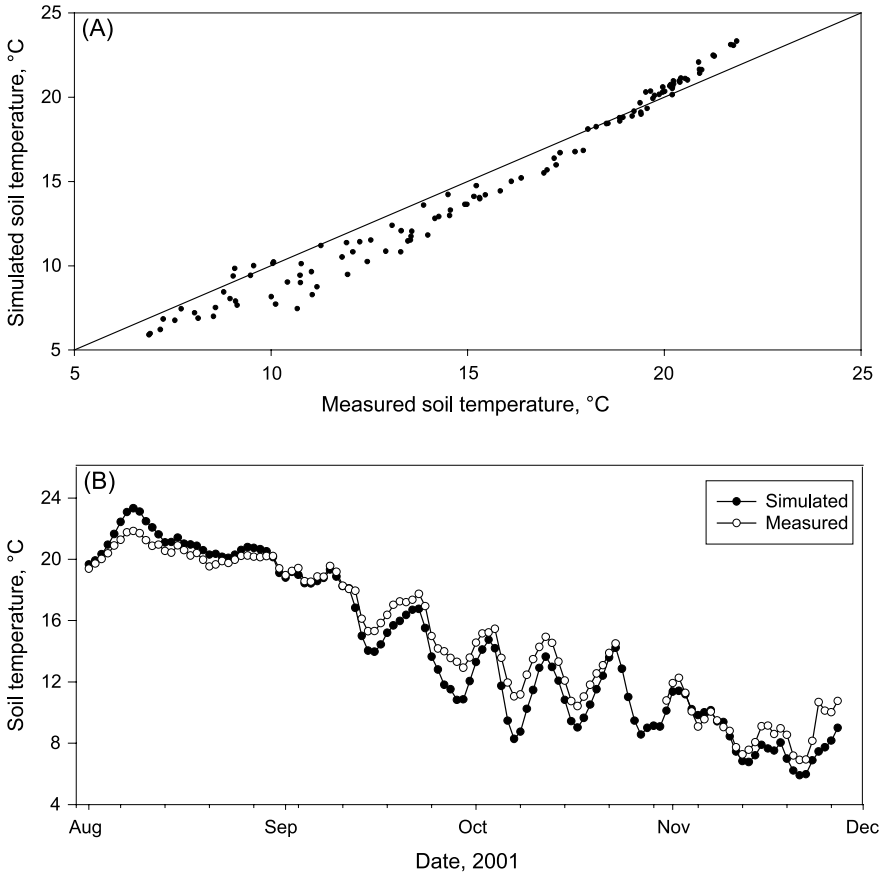

Figure 2. (A) Measured versus modeled soil temperature from site 1, at depth of 20 cm. (B) Measured and simulated soil temperature for site 1 at depth of 20 cm through time.

Spatial patterns of simulated soil tension vary with the overall moisture status for the catchment. On day 7 (10 September 2001), average catchment tension is low (18 cm), as the catchment has just been subjected to a large storm the previous day, so simulated soil tensions are not highly variable (Figure 5A). On day 26 (14 September 2001), the average catchment tension is much higher (103 cm) and it is clear that the hillslopes and ridges are much drier than the hollows and stream channels (Figure 5B).

Soil CO_2 concentration

At site 1, the simulated soil CO_2 concentration data track the modeled data fairly well, with the exception of the month of August when the model significantly overpredicts CO_2 concentrations (Figure 6). The average error of the simulation is

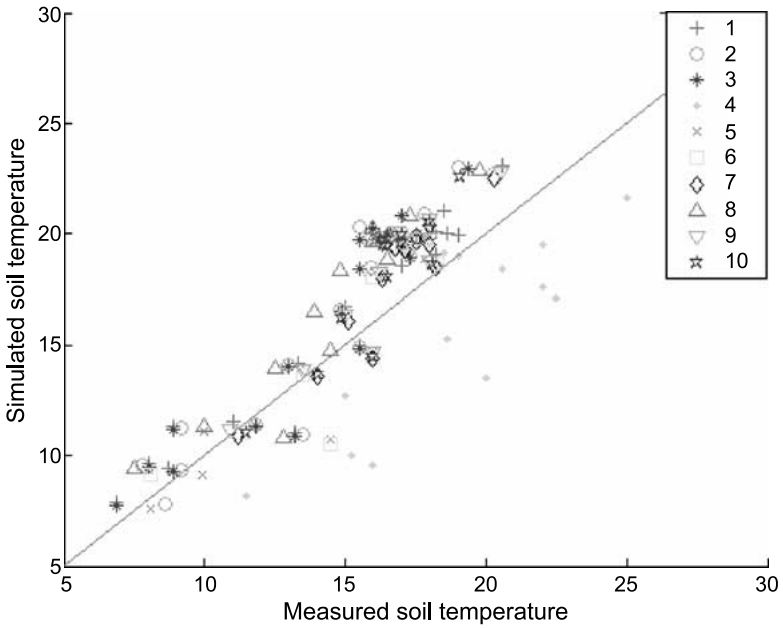

Figure 3. Measured versus simulated soil temperature for each of 10 spatially distributed wells.

2702 ppm CO_2 and the Nash–Sutcliffe criterion is −1.87. When the overpredictions early in the simulation are ignored, the average error decreases to 645 ppm CO_2 and the efficiency increases to 0.56.

For the spatial data, there is close agreement between measured and simulated CO_2 values for the shallow gas wells at low concentrations, but as the concentrations increase, the differences increase (Figure 7). For the shallow gas wells, the average error is 338 ppm CO_2 and the Nash–Sutcliffe criterion is 0.23. A similar pattern is seen for data from the wells at 70 cm depth (Figure 8). The average error is −325 ppm CO_2 and the Nash–Sutcliffe criterion is 0.04 (Figure 8).

When the model is run for each pixel in the watershed over the 35 day period, the lowest CO_2 concentrations are seen in the stream channels where saturated conditions prevail. The highest CO_2 concentrations are simulated in the hollows and riparian zones, at times when the soil is warmest (Figure 9). The spatial patterns for the shallow and deep CO_2 concentrations are similar, with the 70 cm deep results averaging about 4000 ppm CO_2 higher than the 20 cm results. During times when soil tension is low (wet soils) and soil temperature is high, CO_2 concentrations are high throughout the catchment, with locally higher values in topographically wet areas (excluding the stream channels). When catchment soils are generally warm, concentrations decrease as elevation increases and soils become cooler and drier (Figure 9A, C). This pattern is in contrast to that seen when soils are generally cool (Figure 9B, D). During these times, CO_2 concentrations are highest in topographic hollows and along the stream.

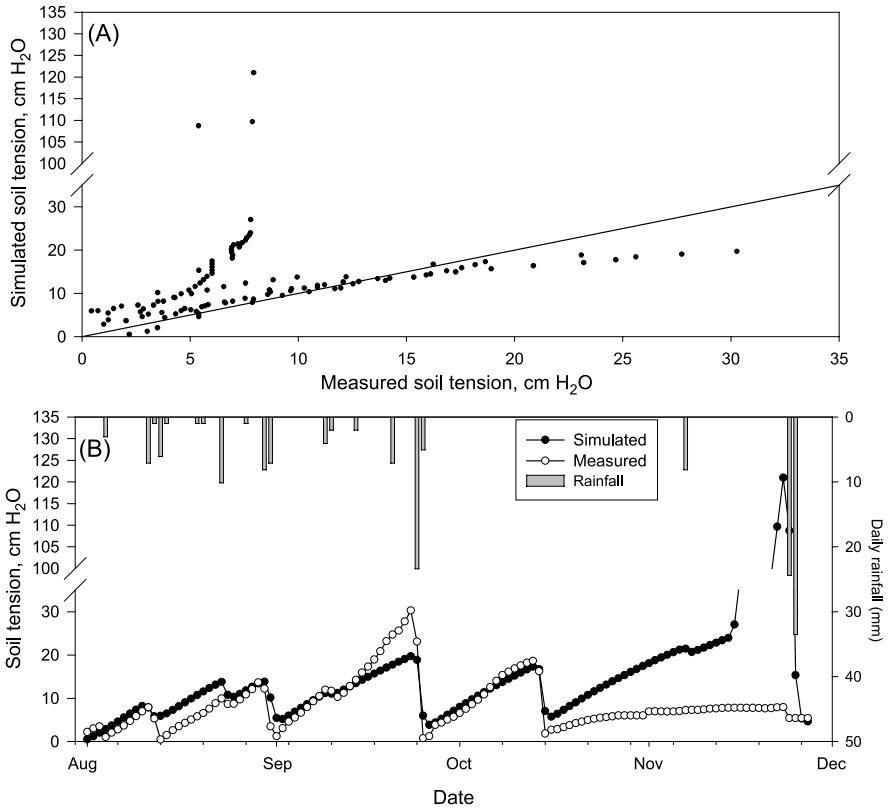

Figure 4. (A) Measured versus simulated soil tension from site 1, at depth of 20 cm. (B) Measured and simulated soil tension at 20 cm from site 1 through time and daily precipitation. Note scale break.

The CO_2 concentration in soils can be large despite respiration being low. This is seen on day 29 in the simulation (26 September) (Figure 10). The rainfall on that day caused a decrease in the diffusivity of the soil such that CO_2 produced through respiration was unable to leave the soil. Because of this, CO_2 remained in the soil resulting in elevated concentrations despite low respiration because of cold soils.

Discussion

Soil temperature

The average difference between simulated and observed data for the spatially distributed soil temperature simulation is larger than that for the calibration data set. One explanation lies in the use of lumped values to represent an obvious

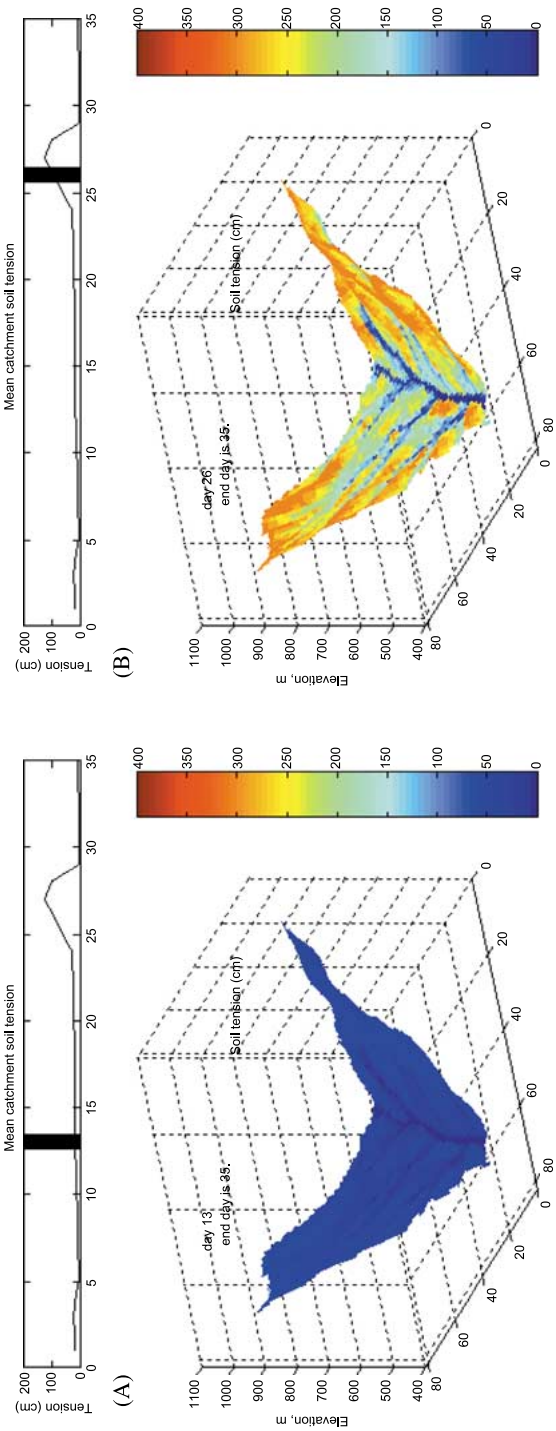

Figure 5. Spatially distributed soil tension for a wet day (A, 7 September 2001) and dry day (B, 14 September 2001) in the simulation. *X* and *Y* axis values are numbers of pixels. Each pixel is 30 m on a side. A colour version of this figure can be found in the online edition of this article.

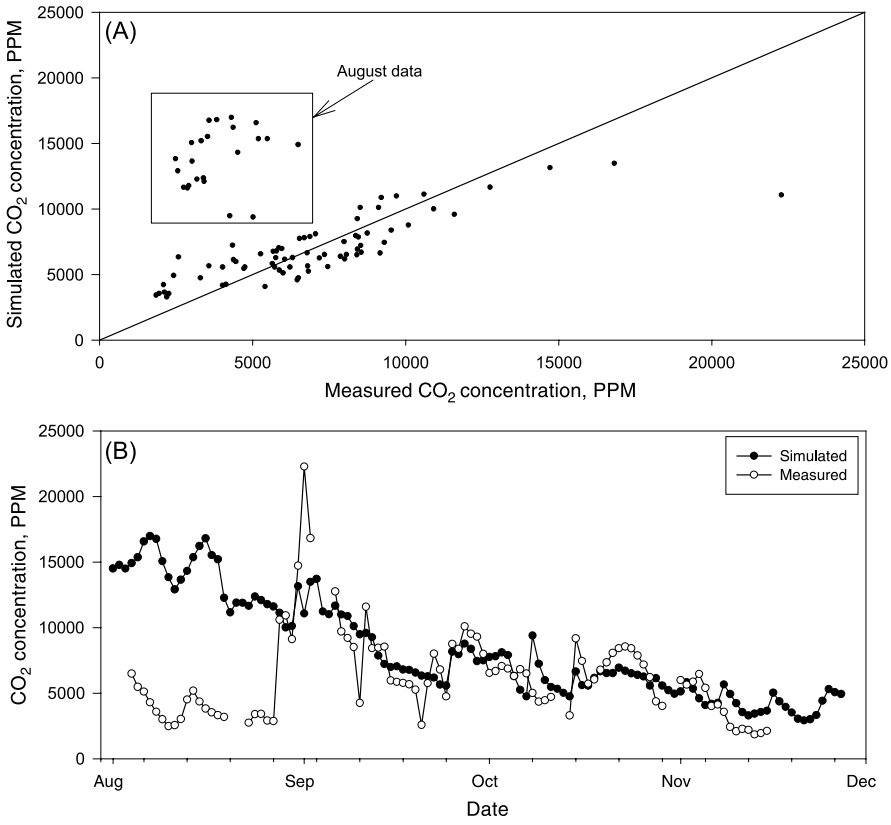

Figure 6. (A) Measured versus simulated soil CO_2 concentration at 20 cm from site 1. (B) Measured and simulated soil CO_2 concentrations from 20 cm from site 1 through time.

spatially variable parameter. LAI varies through the catchment due to ice damage but is considered lumped in the simulations. The soil temperature model systematically under predicted soil temperature at site 4, which is the site with the highest elevation and should theoretically have had the lowest soil temperatures (Figure 3). Site 4 continuously had the highest daytime soil temperatures because it was located in an area of almost no canopy, receiving full solar radiation. Site 4 also had very little litter because of wildfire in the catchment in September 2000, resulting in a low litter LAI.

Soil tension

We assumed a strong relationship between topographic position and soil wetness. However, field investigations have not found this linkage to be nearly as strong as we assume here (e.g., Western et al. 1999). Even with this understanding, it is still

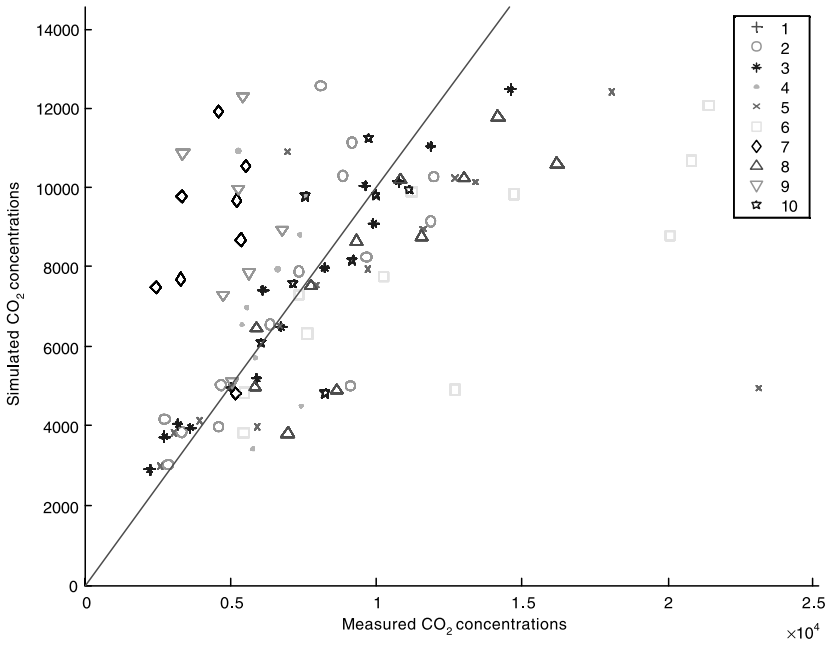

Figure 7. Measured versus simulated soil CO_2 concentrations at 20 cm depth from each of 10 spatially distributed soil gas wells measured weekly from 28 August 2001 to 27 November 2001.

clear that soils in the hollows will be wetter than on slopes, and soils after a storm will be wetter than during a long dry period. Both of these spatial and temporal variations are represented in the simulations utilized here (Figure 5).

We are able to simulate the overall pattern seen in measured soil tension, but we are not able to reproduce accurately the extreme wet and dry end of the tension gradient (Figure 4). This is particularly evident late in the study period beginning on 15 October. Measured tension stays low (soils stay wet) despite the extended lack of rainfall, most likely due to reduced evapotranspiration (ET). During this same period, the hydrological simulation has the soil drying to the highest tensions seen in the study period. TOPMODEL continuously drains the soil during extended dry periods, resulting in very high saturation deficits that are inconsistent with measurements. The impact of this model failure is limited because it occurs at a time of low soil temperatures. Soil water status is not nearly as important for the CO_2 simulation late in the season when ET is low, as during the growing season, when the tension simulations adequately reproduce the measured data.

Soil CO_2 concentrations

The relative importance of soil water and temperature on respiration has been discussed extensively in the literature (e.g., Edwards 1975; Orchard and Cook

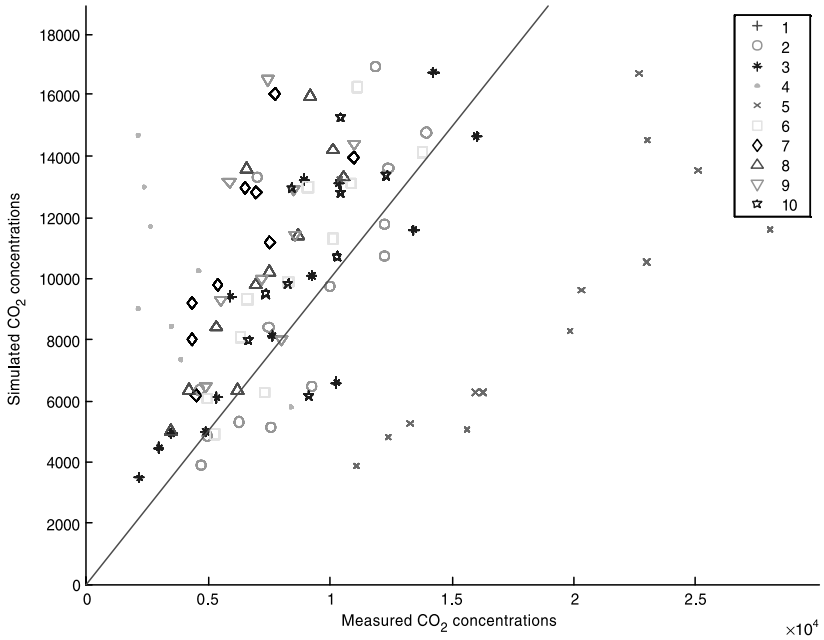

Figure 8. Measured versus simulated soil CO_2 concentrations at 70 cm depth from each of 10 spatially distributed soil gas wells measured weekly from 28 August 2001 to 27 November 2001.

1983; Schlentner and Van Cleve 1985; Howard and Howard 1993; Davidson et al. 1998; Lomander et al. 1998; Fang and Moncrieff 2001). Soil temperature is generally reported to be the dominant control with soil moisture being important, although to a lesser extent (Davidson et al. 1998; Fang and Moncrieff 2001). Our work has shown that, at least during the growing season, soil water content is the dominant control on soil CO_2 concentration, as the soils are thoroughly warmed and temperature is not limiting (Figure 11).

The model adequately simulates most of the time series of measured CO_2, but it overpredicts to a large extent the month of August (Figure 6). The simulated fluxes from the model are high throughout August. So, the problem of overprediction of concentrations must stem from overprediction of respiration. The influence of tension on soil respiration in the model is logarithmic (Šimůnek and Suarez 1993). During the period of overprediction, observed tensions are below 15 cm of water, a value which results in the $f(w)$ term in the model (influence of water on respiration, maximum of 1, Eq. (12)) at 0.6 or above. During this time, the soils are the warmest of the entire simulation, averaging about 21 °C. With high temperatures and moist soils, the model produces high respiration rates. Something is incorrectly specified in the model or not accounted for at all. One possibility is that the high soil temperatures may limit respiration through enhanced drying of the soils, although studies investigating the influence of soil temperature on respiration have not found a point at which this occurs (Davidson et al. 1998; Fang and Moncrieff 2001).

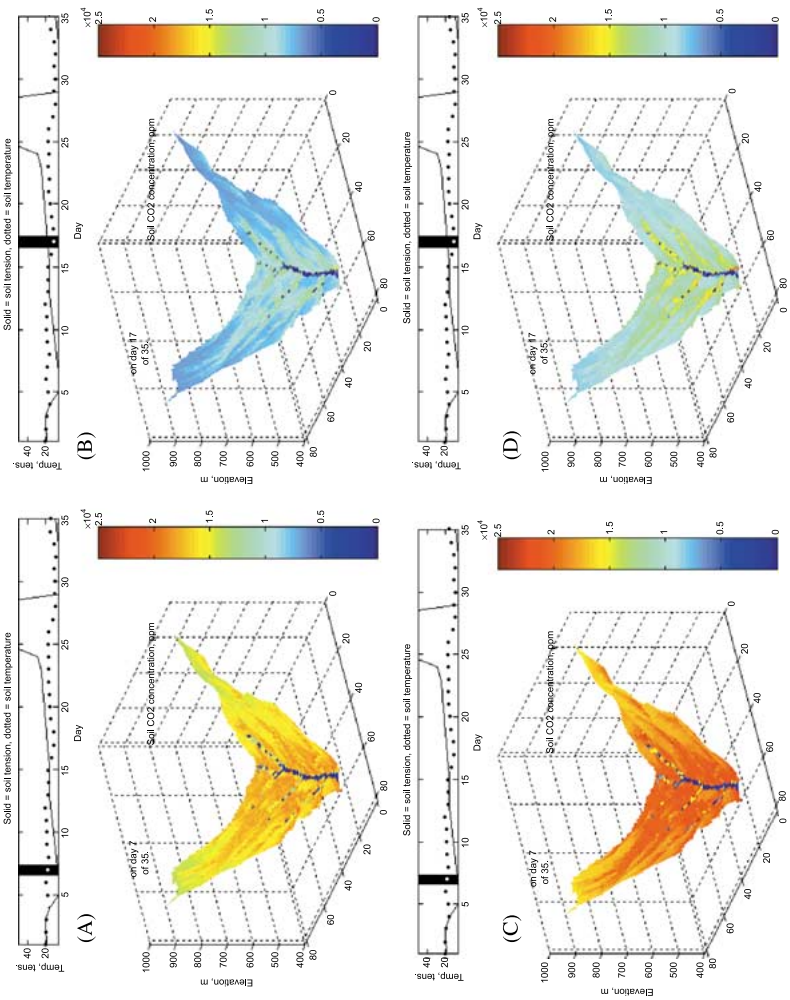

Figure 9. Spatial plots of soil CO_2 concentrations at 20 cm (A, B) and 70 cm (C, D) on a wet day (A, C, 7 September 2001) and a dry day (B, D, 14 September 2001). *X* and *Y* axis values are numbers of pixels. Each pixel is 30 m on a side. A colour version of this figure can be found in the online edition of this article.

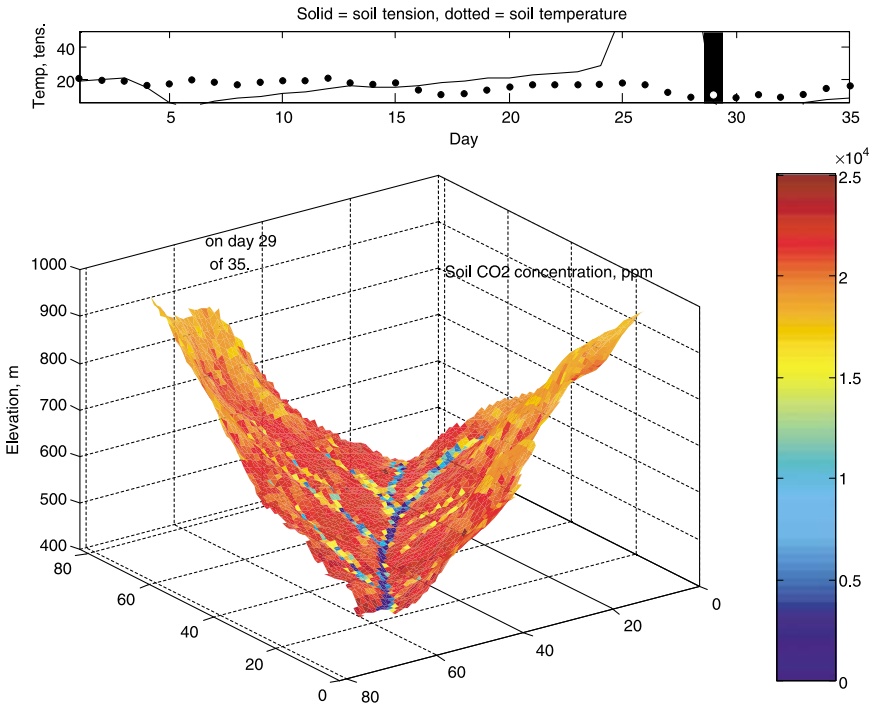

Figure 10. Simulated CO_2 concentrations at 20 cm depth on day 29 (26 September 2001). CO_2 concentrations are high despite low respiration because of cold soils. *X* and *Y* axis values are numbers of pixels. Each pixel is 30 m on a side. A colour version of this figure can be found in the online edition of this article.

The spatial simulations of CO_2 concentrations routinely under predict the shallow CO_2 concentration at site 6 (Figure 7). A possible explanation for the under prediction is that site 6 has very fertile soils which result in higher density of fine roots, causing there to be more substrate for respiration. This is evidenced by the large yellow poplars (*Liriodendron tulipifera*) on the site, a tree known for colonizing rich soils. When soil organic carbon in the model is increased by 50%, data from site 6 falls much closer to the 1:1 line, giving an average error for the shallow soil simulation of 1159 ppm CO_2 and increasing the Nash–Sutcliffe criterion from 0.31 to 0.46.

In both the shallow and deep simulations, CO_2 concentrations at site 4 are over predicted (Figures 7 and 8). Site 4 has limited canopy cover and receives direct incoming radiation, resulting in higher soil temperatures and higher soil tension (drier soils). The higher temperatures would ordinarily be responsible for higher respiration, but the very dry soils overwhelm this effect, causing in low measured CO_2 concentrations at site 4. Site 4 is represented in the model as having cool soil temperatures due to high elevation and as having relatively dry conditions, being near the ridge top. These two factors together result in relatively low predicted CO_2 concentrations (4000–14,000 ppm). However, the observed concentrations are

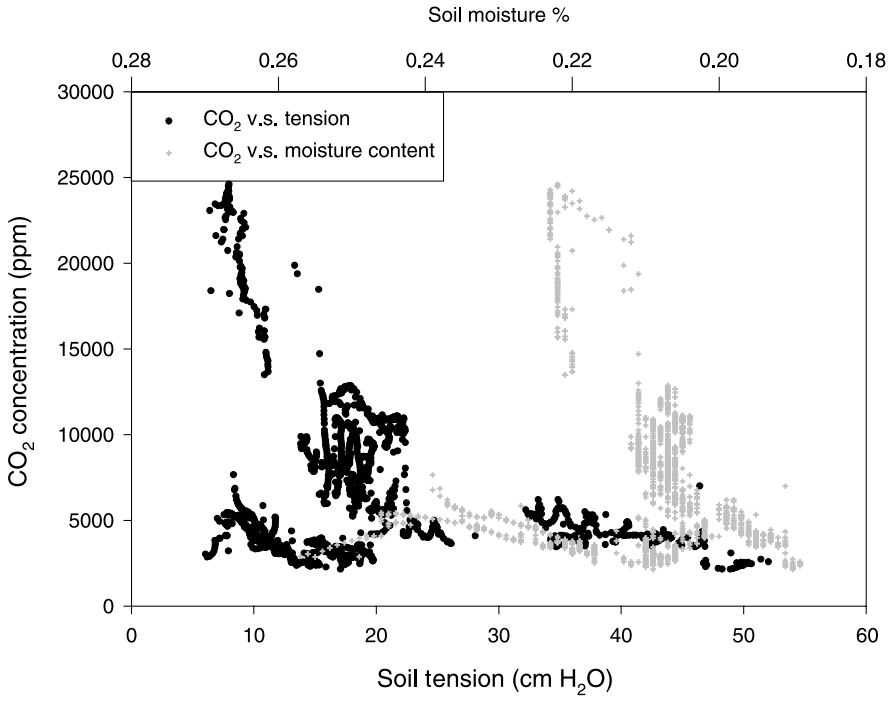

Figure 11. Soil tension and volumetric soil water content versus soil CO_2 concentration at 20 cm depth from site 1.

much lower (2000–5000 ppm, Figure 8). The influence of increased evaporation from exposed soils is not represented in the model and thus causes errors in the predictions.

The CO_2 portion of the model is sensitive to two different sets of parameters. The first set is the respiration rate coefficients which define the optimal rates for root and microbial respiration at 10 °C. The values determined by calibration in this study are 12×10^{-6} and 12×10^{-5} mg CO_2 g^{-1} s^{-1} for microbial and root respiration, respectively. These values are on the same order as those used by Moncrieff and Fang (1999) (3.85×10^{-6} and 4.30×10^{-5} mg CO_2 g^{-1} s^{-1}) for their work in a pine plantation in Florida. Changing the optimal respiration rates has the effect of shifting the entire simulated CO_2 time series up (increased values) or down (decreased values).

The other set of parameters to which the model is sensitive is the tension specifications for setting the influence of water on respiration. Three values must be specified here; the tension where respiration ceases because the soil is to wet (h_1), the tension at which respiration is optimal (h_2), and the tension where respiration ceases because the soil is too dry (h_3) (Eq. (13)). The values used in this study are 1, 25, and 400 cm H_2O for h_1, h_2, and h_3, respectively. Suarez and Šimůnek (1993) used values of 100 and 10^7 cm H_2O for h_2 and h_3. h_1 was not specified but is noted

as being equal to the air entry pressure (Suarez and Šimůnek, 1993). These values are notably higher than those in our simulation. Suarez and Šimůnek (1993) took their values from laboratory experiments investigating *Actinomycetes* growth in sands (Williams et al. 1972). The climate at Brokenback Run is humid and warm, and soils are predominantly clay-loams. These factors result in much lower soil tensions than seen in the sands used by Suarez and Šimůnek (1993).

Conclusion

In this study we present the development and application of a model that is capable of predicting the concentration of CO_2 in soils of a small watershed through both space and time. This tool allows us to address the spatial and temporal variability in soil CO_2 processes as a first step in solving the problem associated with upscaling from points to coarser scales. The ability to accurately predict the amount of CO_2 produced in the soil, the amount leaving the soil through surface efflux, and the concentration in the soil would contribute to an understanding of potential effects on the carbon cycle associated with land use change, climate change, and changes in soil solution chemistry. We have shown that a sequence of fairly simple models can capture major aspects of phenomena that determine CO_2 production rates and concentrations across a catchment.

References

Andrews J. and Schlesinger W. 2001. Soil CO_2 dynamics, acidification, and chemical weathering in a temperate forest with experimental CO_2 enrichment. Global Biogeochem. Cycle 15: 149–162.

Beven K. and Kirkby M. 1979. A physically based variable contributing area model of basin hydrology. Hydrol. Sci. Bull. 24: 43–69.

Campbell G. 1985. Soil Physics with Basic; Transport Models for Soil–Plant Systems. Elsevier, New York.

Castelle A. and Galloway J. 1990. Carbon dioxide dynamics in acid forest soils in the Shenandoah National Park, Virginia. Soil Sci. Soc. Am. J. 54: 252–257.

Davidson E., Belk E. and Boone R. 1998. Soil water content and temperature as independent or confounded factors controlling soil respiration in a temperate mixed hardwood forest. Global Change Biol. 4: 217–227.

Edwards N. 1975. Effects of temperature and moisture on carbon dioxide evolution in a mixed deciduous forest floor. Soil Sci. Soc. Am. Proc. 39: 361–365.

Fang C. and Moncrieff J. 1999. A model for soil CO_2 production and transport 1: model development. Agric. For. Meteor. 95: 236–255.

Fang C. and Moncrieff J. 2001. The dependence of soil CO_2 efflux on temperature. Soil Biol. Biochem. 33: 155–165.

Fang C., Moncrieff J., Gholz H. and Clark K. 1998. Soil CO_2 efflux and its spatial variation in a Flordia slash pine plantation. Plant Soil 205: 135–146.

Howard D. and Howard P. 1993. Relationships between CO_2 evolution, moisture content, and temperature for a range of soil types. Soil Biol. Biochem. 25: 1537–1546.

Kang S., Kim S., Oh S. and Lee D. 2000. Predicting spatial and temporal patterns of soil temperature based on topography, surface cover, and air temperature. For. Ecol. Manag. 136: 173–184.

Lomander A., Katterer T. and Andren O. 1998. Carbon dioxide evolution from top and subsoil as affected by moisture and constant and fluctuating temperature. Soil Biol. Biochem. 30: 2017–2022.

McFee W. and Kelly M. (eds) 1995. Carbon Forms and Functions in Forest Soils. Soil Science Society of America, Madison, 594 p.

Moncrieff J. and Fang C. 1999. A model for CO_2 production and transport 2: application to a Flordia *Pinus elliotte* plantation. Agric. For. Meteor. 95: 237–256.

Orchard V. and Cook F. 1983. Relationship between soil respiration and soil moisture. Soil Biol. Biochem. 15: 447–453.

Rout S. and Gupta S. 1989. Soil respiration in relation to abiotic factors, forest floor litter, root biomass, and litter quality in forest ecosystems of Siwaliks in northern India. Aecta Oecologica Oecol. Plant. 10: 229–244.

Scanlon T., Raffensperger J., Hornberger G. and Clapp R. 2001. Shallow subsurface storm flow in a forested headwater catchment: observations and modeling using a modified TOPMODEL. Water Resour. Res. 36: 2575–2586.

Schlentner R. and Van Cleve K. 1985. Relationships between CO_2 evolution from soil, substrate temperature, and substrate moisture in four mature forest types in interior Alaska. Can. J. For. Res. 15: 97–106.

Šimůnek J. and Suarez D. 1993. Modeling of carbon dioxide transport and production in soil 1. Model development. Water Resour. Res. 29: 487–497.

Suarez D. and Šimůnek J. 1993. Modeling of carbon dioxide transport and production in Soil 2. Parameter selection, sensitivity analysis, and comparison of model predictions to field data. Water Resour. Res. 29: 499–513.

Thunholm B. 1990. A comparison of measured and simulated soil temperature using air temperature and soil surface energy balance as boundary conditions. Agrico. For. Meteor. 53: 59–72.

Vose J. and Swank W. 1991. A soil temperature model for closed canopied forest stands. U.S. Department of Agriculture Research Paper SE-281.

Western A., Grayson R., Blöschl G., Willgoose G. and McMahon T. 1999. Observed spatial organization of soil moisture and its relation to terrain indices. Water Resour. Res. 35: 797–810.

Williams S., Shameemullah M., Watson E. and Mayfield C. 1972. Studies on the ecology of actinomycetes in soil – VI. The influence of moisture tension on growth and survival. Soil Biol. Biochem. 4: 215–225.

Winkler J., Cherry R. and Schlesinger W. 1996. The Q_{10} relationship of microbial respiration in a temperate forest soil. Soil Biol. Biochem. 28: 1067–1072.